International Journal of Thermal Sciences 49 (2010) 143–152

Contents lists available at ScienceDirect

International Journal of Thermal Sciences

journal homepage: www.elsevier.com/locate/ijts

Applications of genetic neural network for prediction of critical heat flux

Huiming Wei, G.H. Su*, S.Z. Qiu, Weifeng Ni, Xingbo Yang

Department of Nuclear Science and Technology, State Key Laboratory of Multiphase Flow in Power Engineering, Xi'an Jiaotong University, Xi'an 710049, China

ARTICLE INFO

Article history:
Received 4 November 2008
Received in revised form
3 June 2009
Accepted 24 June 2009
Available online 3 August 2009

Keywords:
Critical heat flux
Genetic neural network
Genetic algorithm
Prediction

ABSTRACT

In this study, the data set of the 2006 CHF look-up table is partitioned into five subsets by using Fuzzy c-means (FCM) clustering algorithm. The elements of the same subset are 'similar' to each other in some sense while those assign to different subsets are 'dissimilar'. At the same time, a Genetic Neural Network (GNN) model for predicting critical heat flux (CHF) is set up. It has some advantages of its globe optimal searching, quick convergence speed and solving non-linear problem. The methods of establishing the model and training of GNN are discussed particularly in the article. Local condition type CHF is predicted by GNN on the basis of 6930 CHF data from the 2006 CHF look-up table. The prediction results are consistent with database very well. Next, the mainly parametric trends of the CHF are analyzed by applying GNN. At last, prediction of dryout point is investigated by GNN with distilled water flowing upward through narrow annular channel with 0.95 mm and 1.5 mm gaps, respectively. The prediction results by GNN have a good agreement with experimental data. Simulation and analysis results show that the network model can effectively predict CHF.

1. Introduction

Critical heat flux (CHF) is one of the most important quantities when considering the safety limits of nuclear reactors, steam generators and other thermal units. If a heated surface is cooled by a fluid under nucleate boiling condition, the heat transfer coefficient is relatively high and a large amount of heat can be removed with small temperature difference between the wall and fluid. However, this excellent characteristic of heat transfer is not boundless. The heat flux cannot increase indefinitely. At some condition, the steam produced leads to the formation of a continuous vapor film over the surface which may cause the destruction of the heater due to a sudden increase of the surface temperature. The pressurized water reactors (PWRs) shall be designed with sufficient thermal (power) margin for the specifically acceptable fuel design limits to ensure that they are operated safely within the limiting conditions for operation. The limitation is produced from the analysis of CHF. At the CHF point, there is a sharp decrease of the coolant heat transfer coefficient, which would result in the high cladding temperature and the probable failure of nuclear fuel. Due to the complex behaviors of many variables, no deterministic theory exists until now for the prediction of the CHF except approximation from experimental data to design a specific type of nuclear fuel. The uncertainty of the CHF experimental data is very broad because of the uncontrollable parameters such as turbulent flow, surface roughness and fabrication tolerances of test section [1]. It directly affects the thermal margin of nuclear power plants.

Reactor thermal hydraulic designers have developed and updated the CHF correlations to find a best-fit function by conventional regression analysis and trial-and-error-based function model search. We need to understand the effects of many input variables on the CHF in selecting a function model or deriving an equation. Generally, they are analyzed on the basis of an empirical correlation from experimental data by using some physical knowledge [2–5]. Another approach is the CHF look-up table which has been widely adopted due to its accuracy or the widely applicable ranges [6]. Recently, advanced approaches to improving CHF prediction in simple geometry have been studied. In reference [7], the alternating conditional expectation algorithm, a kind of nonparametric regression method, was used to generate correlations automatically. It tries to find an optimal transformation of variables and then simple regression analysis is performed for the transformed variables. In reference [8], genetic programming was used to find a mathematical expression in a symbolic form between dependent and independent variables. Hundreds of different models and correlations on the prediction of CHF exist in the open literature and enormous amounts of experimental data are available at present. Most of the studies carried out on CHF have been reviewed in various publications. The work of Katto [9] is particularly interesting as he deals with the CHF phenomenon specifically

* Corresponding author. Tel./fax: +86 29 82663401.
E-mail address: ghsu@mail.xjtu.edu.cn (G.H. Su).

1290-0729/$ – see front matter © 2009 Elsevier Masson SAS. All rights reserved.
doi:10.1016/j.ijthermalsci.2009.06.007

Nomenclature

A_i	the ith prediction signal
BP	back-propagation
CHF	critical heat flux (kW m^{-2})
d_{jk}	the distance from x_j to V_k
dH	hydraulic diameter
FCM	fuzzy c-means
$F(\cdot)$	the activation function
F_{fitness}	fitness function
F_i	the fitness of ith individual
G	mass flow velocity (kg m^{-2} s^{-1})
GA	genetic algorithm
GNN	genetic neural network
h_{fg}	latent heat (J kg^{-1})
J_{m}	the sum of objective function
L	heated length (m)
m	weighting exponent
P	pressure (MPa)
P_i	the selection probability of ith individual
q_{cal}	calculation critical heat flux (kW m^{-2})
q_{data}	data set critical heat flux (kW m^{-2})
q_{exp}	experimental critical heat flux (kW m^{-2})
q_{pre}	prediction critical heat flux (kW m^{-2})
T_i	the ith goal signal
V_k	the cluster center of the kth cluster
w_k	synaptic weights of neuron
W_i	the ith weight gene of chromosome
x_{p}	the pth input signal
X	a finite set of data
x	critical quality
$\|\cdot\|$	inner product induced norm metric

Greek letters

ϕ	the membership matrix
$\phi^{(\tau)}$	the τ iterative membership matrix
φ_{kj}	the membership degrees of the datum x_{j} in class k
θ	threshold
θ_j	the jth threshold gene of chromosome

in both internal and external flows and presents a valuable reference on this subject.

Fuzzy c-means (FCM) clustering algorithm [10] is one of most important and popular fuzzy clustering algorithms. It is a widely applied method for acquiring fuzzy pattern from data set [11]. Its aim is to partition a set of unlabeled data set into c subsets. The elements of each subset are 'similar' [12]. Therefore, FCM cannot only obtain more clustering information, but also reflect more accurately the actual distributing characteristic of data. We can analysis more accurately the characteristic of these data. There are two main approaches to clustering. One method is hard clustering; the other one is fuzzy clustering. However, a characteristic of the hard clustering method is that the boundary between clusters is fully defined. In a realistic case, the boundaries between clusters cannot be clearly defined. Therefore, the fuzzy clustering method is usually adopted to classify these patterns.

Genetic algorithm (GA) is a powerful optimization technique inspired by the natural selection principles and Darwin's species evolution theory [13]. Because of their robustness and easy customization for different kinds of optimization problems, GA has been successfully used in a wide range of engineering applications. Compared to the conventional optimization methods that move from one point to another, GA starts from many points simultaneously climbing many peaks in parallel. Therefore, it is less susceptible to be stuck at local minima than conventional search methods [14,15]. Also, it is the most useful method [16–19] to solve optimization problems with multiple objectives. The optimization parameters are encoded into symbolic structures, metaphorically called genotypes that carry intrinsic characteristics of the symbolic individual. As the generation proceeds, populations of chromosomes are iteratively altered by biological mechanisms inspired by natural evolution such as selection, crossover and mutation. Then, from generation to generation, the average fitness of the individuals increase, evolving the population to its optimum adaptation. The GA starts the adaptation process from a random generated population of individuals. Then, each individual is assigned a fitness that predicts its adaptability, finally, natural selection, crossover and mutation are simulated. The selection probability of a given individual is a function of its fitness. The crossover is made by choosing a random point of the binary string that represents the genotype, followed by the change of parts between the two parents. The mutation is simulated by the inversion of one of the bits of the genotype according to the mutation probability that is a genetic parameter.

At present, BP neural network [20–23] is widely used because it can effectively solve non-linear problem. However, there are some shortcomings for BP neural network, such as slow convergence and easily deep in local extreme point. This is very disadvantageous under limited experiment data of CHF. In order to reduce experiment times and improve reliability of network, the present paper adopts a method to integrate genetic algorithm and neural network and use genetic algorithm to optimize network weight and threshold [24–29]. The shortcoming is solved and the weight and threshold are optimized. The accurate degree of predicting CHF data is achieved by GNN.

In general, CHF correlations are applicable to specific geometries and cover specific ranges of system parameters. They cannot be expanded into conditions far beyond the ranges of their data sets. Besides these approaches, Groeneveld, et al. [6,30] developed a CHF table look-up method which has been widely adopted in several thermal hydraulic computer codes as the standard CHF prediction method because of its accuracy and the widest applicable ranges. It covers the following ranges of flow and geometric parameters: system pressure, 0.1–21.0 MPa; mass flux, 0–8000 kg/m^2 s; steam quality, −0.5–1.0. However, the standard CHF tables are presented for discrete range of pressure, mass flux and steam quality. They are usually normalized for a fixed tube diameter of 8 mm. The CHFs for conditions between the tabulated values are obtained by linear interpolation.

The aim of this study is to propose a new method—GNN to predicate CHF for uniformly heated vertical round tubes within the wide applicable ranges. It has some advantages of its globe optimal searching, quick convergence speed and solving non-linear problem. In this paper, at first, we attempt to classify the CHF data based on the distribution of the experimental conditions and the parametric trends of the CHF values. The classification is accomplished by using fuzzy clustering. It searches the structure in a data set and classifies the CHF data into similar groups for handling these data efficiently. The classification process is necessary to improve the prediction performance of a GNN because the CHF experimental conditions are very broad. The classified CHF data are used to train and test the network. Next, the CHF are predicted by using GNN. We give the comparisons between the database and prediction results of GNN. At the same time, the effects such as

pressure, mass flow rate and equilibrium quality of main parameters on CHF are analyzed using GNN. The results agree with practical behavior as they are generally understood. Finally, GNN is employed to predict the CHF in narrow annuli channels.

It is well known that Groeneveld CHF look-up table has been widely adopted in several thermal hydraulic computer codes as the standard CHF prediction method because of its accuracy and the widest applicable ranges. This work is only an academic work. In this study, we only use the database of Groeneveld CHF look-up table to test the FCM and GNN theory. As an application of GNN, it was used to predict the CHF for distilled water upward flow in vertical narrow annuli with bilateral heating. Therefore, the basic experimental apparatus are briefly introduced in the following section.

2. Experimental apparatus

The experiments were conducted in the following water test loop. Fig. 1 is a schematic of the boiling upward flow system apparatus used in the experiments. The experimental system consists of a pump, pressurizer, pre-heater, calibrated flow meter, condenser, test section, valves and connected pipes. The working fluid is distilled water. Subcooled water is driven by the pump, going through the system pipes, flow meter, pre-heater, the experimental test section, the condenser, and finally returning to the pump after being condensed. The mass flow rate is regulated and maintained by the bypass and the valves. To pressurize the loop, nitrogen gas was injected to the upper part of the pressurizer which provides a compressible volume to the loop for maintaining the desired pressure value.

Test sections are made of specially processed straight stainless steel tubes with linearity error less than 0.01% to form narrow concentric annuli whose electrical and mechanical characteristics were well validated. Fig. 2 shows the diagram of the experimental test section. It has the following geometrical parameters: length in 850 mm; 10 mm inner diameter of the outside tube, 8.1 mm and 7 mm outer diameter of the inside tube. So the corresponding annular gap size is 0.95 mm and 1.5 mm, respectively. The test section is bilaterally heated by AC power supply. In order to ensure the concentricity and the electrical insulation between the outside and inside tubes, the three small ceramic rods are arranged at the same cross section with equal angular interval at the middle of experimental test section. They are shown in Fig. 3. To reduce the heat losses of the experimental test section, the whole experimental test section was firstly covered by silicon–aluminium glass fiber of 120 mm in thickness. At the same time, to compensate heat loss of the experimental test section, a wire heater of 3 kW in maximum power was wrapped outside of this heat insulator. Finally, another silicon–aluminium glass fiber 50 mm in thickness was wrapped outside of the wire heater. Two thermocouples are located in the different places of the inner silicon–aluminium glass fiber along radial direction. Controlling the quantity of compensating heat to make the temperatures of the two thermocouples the same as possible, then good heat insulation could be acquired for the experimental section.

301 experimental data were obtained. The ranges of experimental parameters were as follows:

- heated length (L):0.85 m
- pressure (P): 1.08–3.11 MPa
- mass flux (G): 56.5–141.6 kg m^{-2} s^{-1}
- critical quality (x) : 0.694–0.987.

3. Theories of the classification and GNN

3.1. Fuzzy c-means clustering

In this section, we briefly describe the fuzzy c-means algorithm. In our notation, let $X = \{x_1, x_2, \ldots, x_N\} \subset R^M$, X is a finite set of data in the pattern space which has N patterns. $x_j = (x_{j1}, \ldots, x_{jp}) \in R^M$ is the jth experimental datum, p is the dimension of the pattern vectors. FCM clustering partitions a data set so as to minimize the sum of objective function J_m as follows:

$$J_m = \sum_{j=1}^{N} \sum_{k=1}^{c} \left(\varphi_{kj}\right)^m d_{jk}(x_j, V_k) \tag{1}$$

$$\sum_{i=1}^{c} \varphi_{kj} = 1, \varphi_{kj} \in [0,1], \forall j, d_{jk}(x_j, V_k) = \|x_j - V_k\|^2.$$

where $V_k = (v_{k1}, \ldots, v_{kp})$ is a cluster center of the kth cluster. d_{jk} is the distance from x_j to V_k, which measures the similarity between the

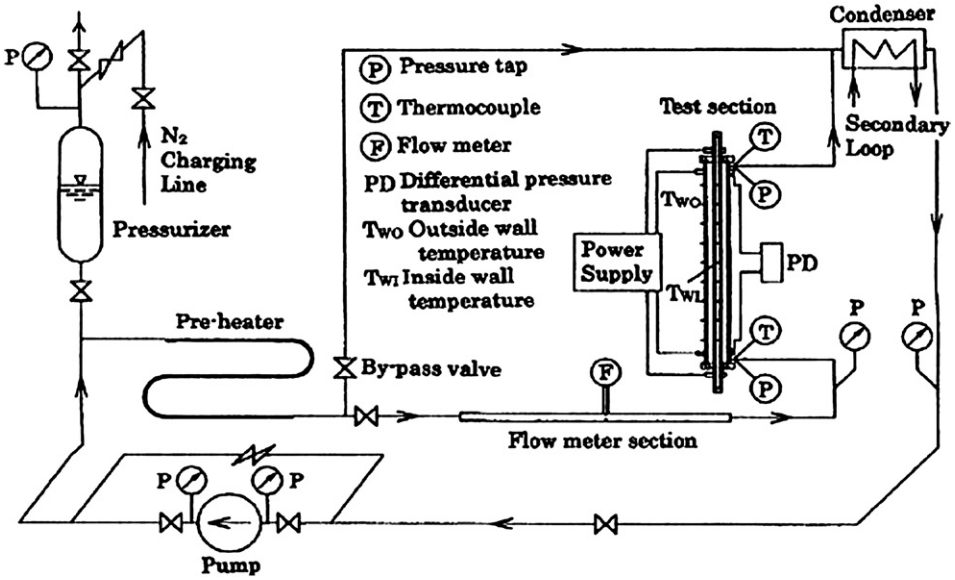

Fig. 1. Schematic of experimental apparatus.

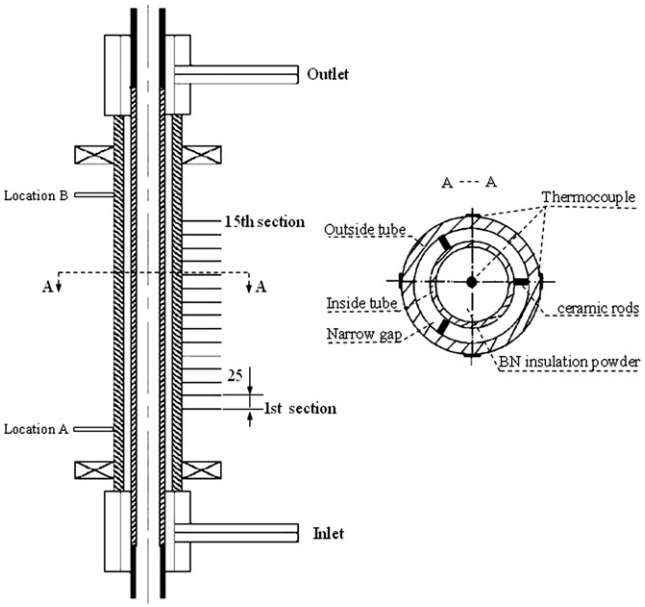

Fig. 2. Schematic of the test section.

datum x_j and the cluster center V_k. The weighting exponent m is the smoothing parameter which represents the fuzziness of clustering. The elements of the membership matrix $\phi = [\varphi_{kj}]_{c\times n}$ represent the membership degrees of the datum x_j in class k. Computer or update the partition matrix $\phi^{(\tau)}$ using the following iterative rule formula for given c and m greater the positive integer 1:

$$\varphi_{kj} = \left[\sum_{i=1}^{c}\left(\frac{d_{jk}}{d_{ji}}\right)^{2/(m-1)}\right]^{-1} \tag{2}$$

$$v_{ij} = \frac{\sum_{k=1}^{n}(\varphi_{ik})^m x_{kj}}{\sum_{k=1}^{n}(\varphi_{ik})^m}, j = 1,\ldots,p \tag{3}$$

The FCM algorithm is shown in Fig. 4. The values of c and m are fixed and any inner product induced norm metric $\|\cdot\|$ can be chosen. In this study, the diagonal norm is selected to measure the similarity of data.

FCM method classifies the database into c clusters via iterative optimization. It iterates until $|\varphi^{(a+1)} - \varphi^{(a)}| < \varepsilon$, that is, the maximum change in membership function between iteration step a and step $a+1$ is within the convergence criterion ε. In order to gain the most valid and optimal clustering of data, the validity and optimality of these partitions are examined by minimizing the compactness and separation validity function S. It is defined as

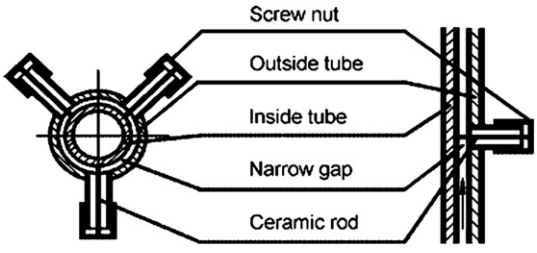

Fig. 3. Schematic description of holding concentricity.

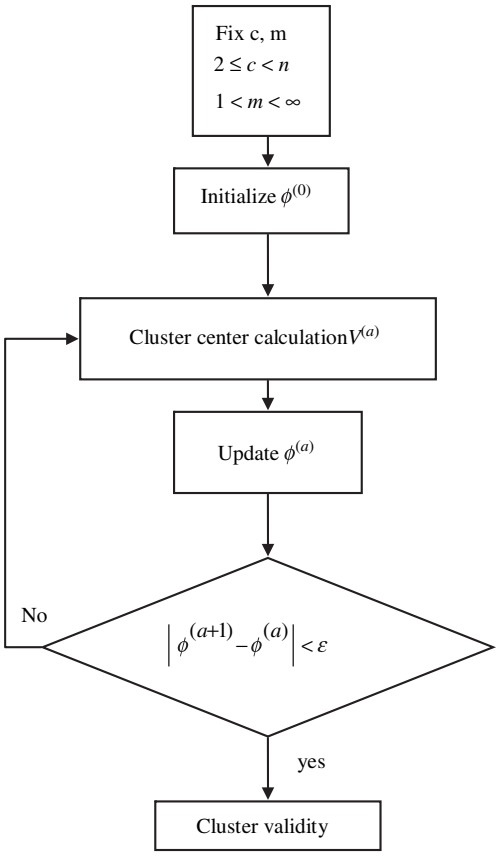

Fig. 4. FCM clustering procedure for the CHF data.

$$S = \frac{\sum_{i=1}^{c}\sum_{j=1}^{N}\left(\varphi_{ij}\right)^m d_{ji}^2}{N\min_{i,j} d_{ji}^2}. \tag{4}$$

It is used as the optimal partition index [31,32] and has a minimum value for the optimal clustering.

3.2. GNN

3.2.1. Structure of the network

A multiple layer neuron network is established to predict CHF. Input layer of the prediction network is responding to CHF parameter. The dimension of input layer can be completely designed according to influence factors on CHF. Output layer of the network is the CHF that will be predicted. The number of hidden layer unit is in direct contract with the predicting precision. Therefore, there must be the best number of hidden layer unit. The initial number of hidden layer unit is determined by using experiential method and the experienced relation which is introduced by Yuan in [33]. In this paper, the dimensions of input and output layers are 3 and 1, respectively. The hidden layer units are 16. Therefore, a single hidden layer BP network can meet need of predicting CHF. Fig. 5 shows the topology of GNN with one hidden layer. The model of each neuron in the GNN includes non-linearity at the output end. We use a common form of non-linearity which is hyperbolic tangent function. Multilayer perceptron is trained in a supervised manner with a highly popular algorithm known as the back-propagation algorithm. It is based on the error-correction learning rule. GNN consist of a great number of neurons which are connected to one another. A neuron is an information-processing unit that is fundamental to the operation of a neural network. Fig. 6

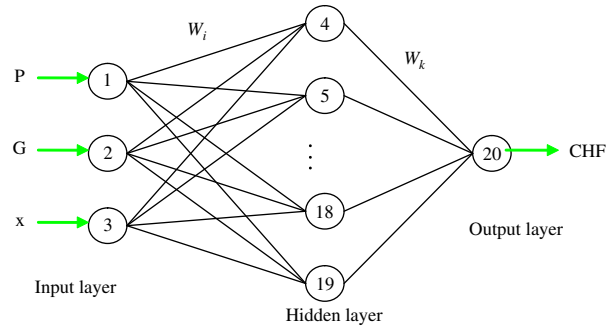

Fig. 5. Structure of genetic neural network.

shows the model for a neuron. In mathematical terms, a neuron is described by the following equation:

$$\text{output} = F\left(\sum_{k=1}^{p} w_k x_k - \theta\right) \tag{5}$$

where $x_1, x_2 \ldots x_p$ are the input signals. $w_1, w_2 \ldots w_p$ are the synaptic weights of neuron. θ is threshold, output is CHF and $F(\cdot)$ is the activation function.

3.2.2. Optimizing network weight and threshold using GA

Genetic operation using colony search technology can be avoided getting into local extreme point. It can solve how to optimize weight and threshold of BP network. It is employed to optimize the weight and threshold of the network in this study. The operation is divided into six sections as follows:

1) Coding of weight and threshold

The input signals should be transformed into genetic genes—chromosome. The model adopts binary coding method. The vector that chromosome responding with weight and threshold of network is:

$$W = [W_1, \ldots, W_i, \ldots, \theta_1, \ldots, \theta_j] \tag{6}$$

where W_i is the ith weight gene of chromosome, θ_j is the jth threshold gene of chromosome.

2) Initialization of population

After coding the weight and threshold of the network, chromosome is yielded at random and makes up an initial population. We start iterative search using initial population as a start point. Finally, population size, selection probability, crossover probability and mutation probability are determined by experiments. They are 80, 0.8, 0.6 and 0.001, respectively.

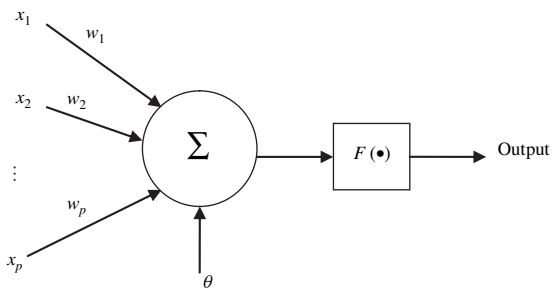

Fig. 6. Neuron model.

3) Fitness function

Fitness function is an important principle on evaluating individual. The Fitness function of the model uses the reciprocal of error squaring sum between prediction signal and goal signal, is as follow:

$$F_{\text{fitness}} = \frac{1}{\sum_{i=1}^{n}(A_i - T_i)^2 + \varepsilon} \tag{7}$$

where n stands for the number of the samples, A_i are prediction signal, T_i is goal signal, ε (>0) is any sufficiently small. The ε is 0.00001 in this study.

4) Selection operation

The selection operation is to choose the individual who has the large fitness from the population. It has the chance to propagate offspring. A roulette wheel selection method is used to choose new individual in this study. Probability of individual selection is:

$$P_i = \frac{F_i}{\sum_{i=1}^{n} F_i} \tag{8}$$

where, P_i and F_i are the selection probability and fitness of ith individual, respectively.

5) Crossover operation

The crossover operation for GA creates variation in the population by producing new offspring that consists of the parts taking from each parent. It is that some genes of two chromosomes are exchanged to produce new individual. In this study, two parental chromosomes and bunch's crossing position are determined by random.

6) Mutation operation

The mutation operation introduces random changes in structure in the population. It is to change some values of chromosomes of weight and threshold with little probability. It cannot only avoid some information be lost perpetually resulting from selection and crossover operation, but also ensure validity of genetic arithmetic. By using the above genetic algorithm operation, appropriate network weight and threshold are obtained. The overall classification, GA optimization, training, learning and prediction procedure for the each cluster of CHF data is represented in Fig. 7.

In brief, genetic algorithms using a variety of coding, recombination, mutation and fitness-based selection strategies may be used to evolve ANN with parameters optimized for predicting problems. Although in many domains genetic algorithms evolved the optimal ANN for predicting problems and they have provided better solutions for optimization problems, there are some limitations. One limitation is that the choice of parameter values for the genetic algorithms (random initial populations of recombinant variables, crossover and mutation rates and number of generations for evolution) and the neural networks (number of hidden layers, number of neurons per hidden layer, learning rates and momentum) may have influenced the CHF predicted and they are determined by many experiments. Another limitation is different procedures evolved the optimal ANN and they are somewhat different. This reinforces the fact that genetic algorithms, while

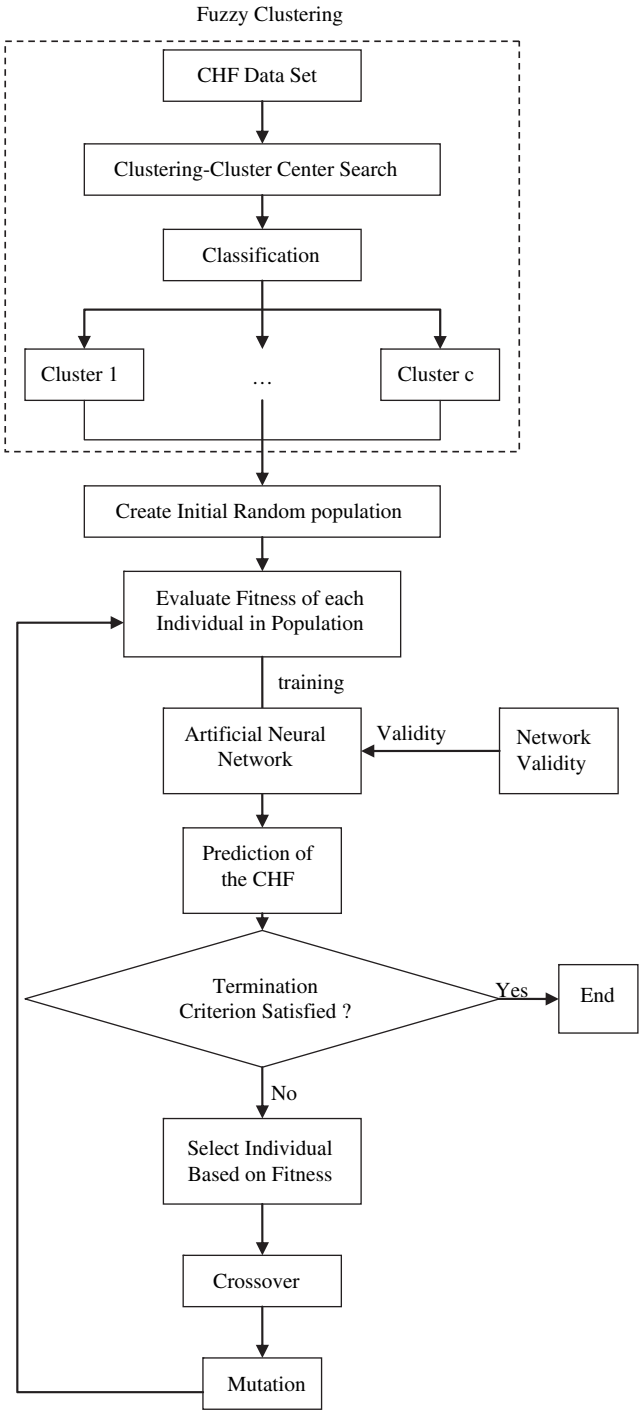

Fig. 7. The overall classification and prediction procedure for the CHF database.

finding good solutions to a prediction problem, may not find the single best solution representing a global minimum on a parameter error surface, since an exhaustive combinatorial search has not been performed [36]. Such algorithms should be further studied on other prediction problems.

4. Fuzzy clustering of the CHF data

The 2006 CHF look-up table [30] was selected as the database in this study. The study is restricted to local conditions type CHF, which is a dependent variable in the CHF experiment. The converted CHF data consist of the relationship of four variables, P, G, x and q. With the CHF data set X [P, G, x, q], the optimal cluster centers are found to have five clusters by using the fuzzy clustering method explained in the prior sections. Through sensitivity study, the weighting exponent m is chosen as 1.25. Five clusters are determined by using fuzzy clustering. The calculated cluster centers are represented in Table 1. By an investigation into the clustered data, each cluster has a characteristic data range as shown in Table 2.

5. Prediction of the CHF

The GNN is trained and tested based on the database. Typically 75% of the each cluster data was used for training and cross validation (60% for training and 15% for cross validation) and the rest 25% for testing. The mean square errors (MSE) of the each cluster training, validation and testing are all lower than 0.04823, 0.06185 and 0.07364, respectively. The prediction results for clusters are represented in Fig. 8. Fig. 8 is the comparison between the database and prediction results of all five clusters by using GNN. From Fig. 8, we can see the prediction results of the local condition type are consistent with experimental data very well. From the results, the MSE are lower than 0.143.

In the following, we compared the results obtained by GNN with other empirical correlations. Kottowski et al. [34] carried out experiments on the CHF for sodium and potassium, derived the following empirical correlation based on 170 data points, including their own data and some others:

$$q_c/GH_{fg} = 0.216(\mathrm{dH}/L)^{0.8}(1-2x)G^{-0.193}. \quad (9)$$

Covering the following ranges of the length/hydraulic diameter ratio L/dH = 30–125, the critical quality $x = -0.4$–0 and the mass flux $G = 50$–800 kg/m^2 s. Fig. 9 shows the results obtained by GNN, which are compared with the calculation data using Kottowski's empirical correlation. Good agreement between the results obtained by GNN and experimental data. They make a great deal of difference between Kottowski's calculation data and experimental data. Different working medium and materials are likely lead to the difference. B&W-2 correlation is derived based on 207 experimental data points:

$$q_{CHF} = 3.155\times10^{-3}(1.155-16.025\,\mathrm{dH})\times\left[3.702\times10^{7}\left(4.3604\times10^{-4}G\right)^{B}-48.21Gxh_{fg}\right]\Big/\times\left[12.71\left(2.252\times10^{-3}G\right)^{A}\right] \quad (10)$$

where $A = 0.712 + 3.006\times10^{-5}$($P$-13790), $B = 0.834 + 9.93\times10^{-5}$($P$-13790).

Covering the following ranges of the system pressure $P = 13790$–16550 KPa, the hydraulic diameter dH = 0.0051–0.0127 m, the critical quality x = −0.03–0.2 and the mass flux $G = 1020$–5425 kg/m^2 s. Fig. 10 shows the results obtained by GNN,

Table 1
Fuzzy cluster centers of the CHF database.

Cluster	P (kPa)	G (kg m^{-2} s^{-1})	x(-)	q (kW m^{-2})
1	16300.1	5273.8	−0.36	20717.3
2	5564.5	1328.9	0.17	3443.6
3	14699.8	4874.5	−0. 15	4908.7
4	3347.2	5832.3	0.31	1499.1
5	1260.3	583.6	0.78	938.9

Table 2
The database of each cluster by fuzzy classification.

Cluster	Number of data	P (kPa)	G (kg m^{-2} s^{-1})	x(-)
1	1604	5000–21000	0–55000	−0.5–0.9
2	482	100–12000	750–8000	−0.5–−0.10
3	1682	500–16000	0–8000	−0.05–0.9
4	1862	100–14000	0–6000	−0.5–0.6
5	1300	3000–21000	2000–8000	−0.5–0.9

which are compared with the calculation data using B&W-2 empirical correlation. They are consistent with experimental data. However, the B&W-2 empirical correlation can only be applied in its experimental parameter ranges. The GNN has the wide applicable ranges. Moreover, the GNN give accurately prediction. The GNN has been applied successfully in the prediction of CHF for upward water flow in vertical round tubes under the wide applicable ranges.

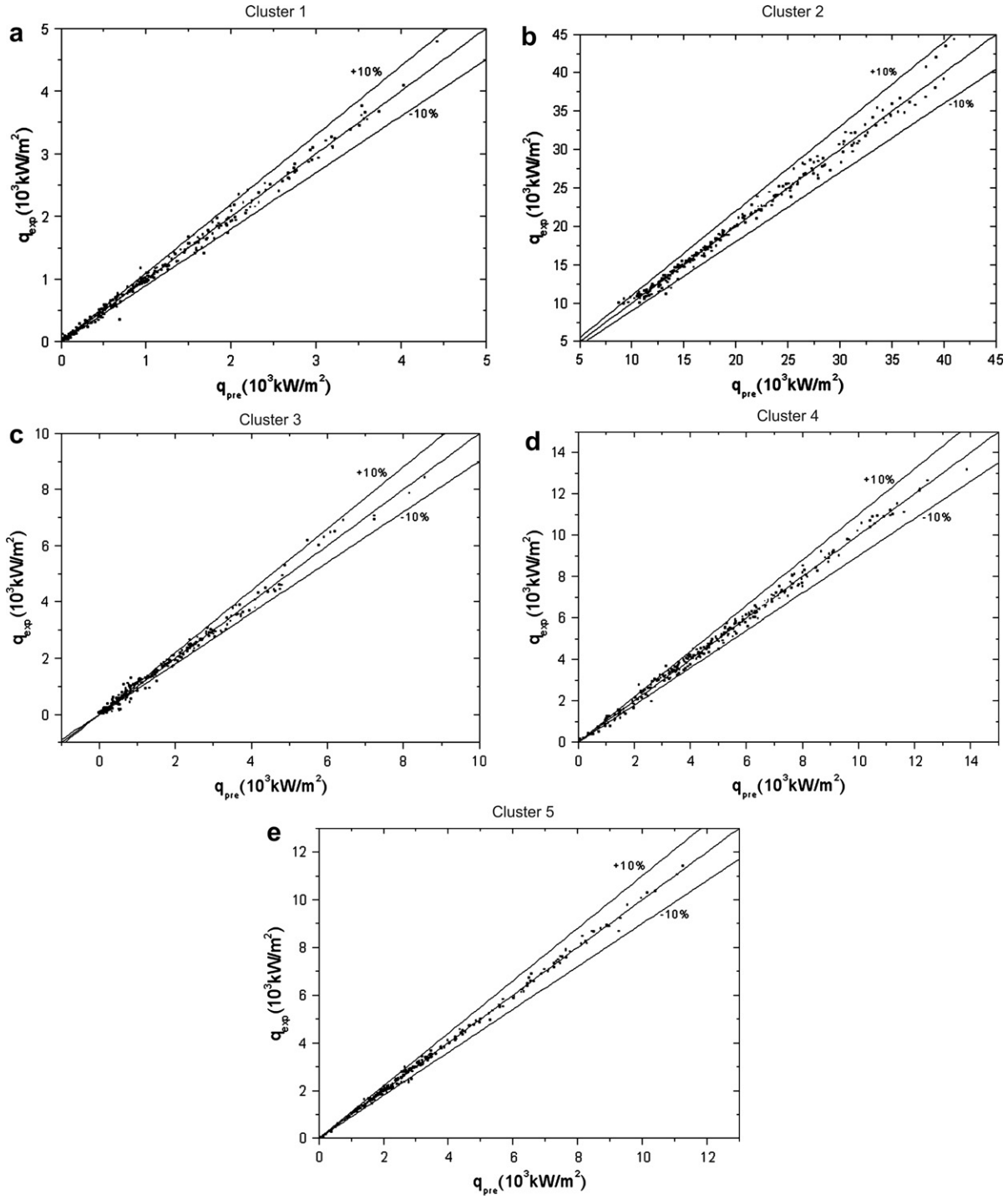

Fig. 8. Comparisons between the Database and Prediction results of the Genetic Neural Network.

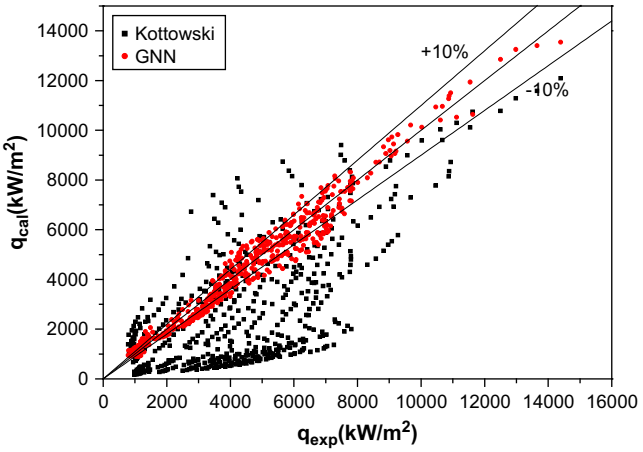

Fig. 9. Comparisons between the Kottowski's Experimental Correlation and the GNN.

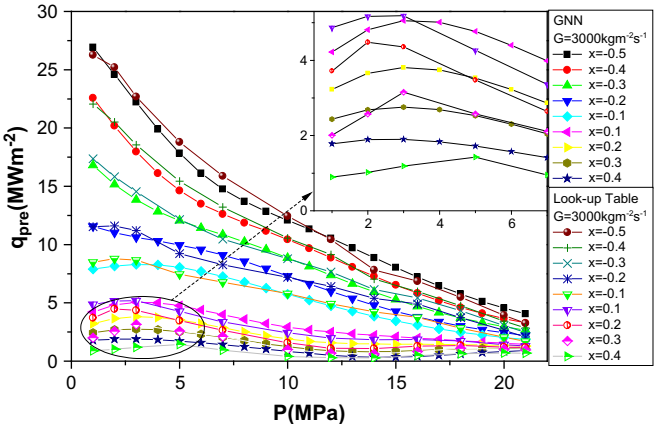

Fig. 11. Effect of system pressure on CHF for local conditions ($G = 3000\ \mathrm{kg\,m^{-2}\,s^{-1}}$).

6. Parametric trends of CHF

In this section, the parametric trends based on local conditions are predicted by using GNN. The local conditions hypothesis is nearly independent of the other variable besides system pressure, mass flux and critical quality. However, it is very useful for the prediction of the CHF in practical applications. The prediction parametric trends are shown in Figs. 11–13. In the figures, the actual outputs of the GNN are simply connected by lines. The trends agree with general understanding. In the following, the parametric trends are discussed.

The overall trend of system pressure is shown in Fig. 11. In this figure, the results obtained by the GNN agree well with the database. Fig. 11 shows the variation of CHF with pressure under local conditions. CHF data are represented for a fixed mass velocities $3000\ \mathrm{kg\,m^{-2}\,s^{-1}}$ and nine different critical qualities over a broad pressure range of 1–21 MPa. From Fig. 11, we can clearly see that the CHF decreases with increasing system pressure under sub-cooled boiling. However, the pressure effect is shown to be complex under nuclear boiling. In overall, the CHF increases with pressure at low pressures, passes through a maximum, then decreases at higher pressures. However it should be noted that the trend is not so clear. The maximum is found at about 4 MPa. From Fig. 11, we can also see that the CHF decreases with increasing critical quality. Moreover, the effect of critical quality with sub-cooled boiling is larger then nuclear boiling.

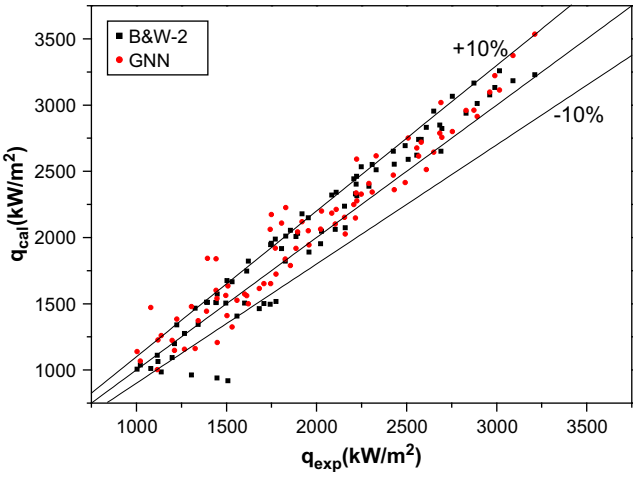

Fig. 10. Comparisons between the B&W-2 Experimental Correlation and the GNN.

The effect of mass velocity on CHF at 10 MPa is represented in Fig. 12 for nine different critical qualities over a broad mass velocity range of 1000–8000 $\mathrm{kg\,m^{-2}\,s^{-1}}$. In this figure, good agreement between the results obtained by the GNN and database was found. Fig. 12 shows the CHF increases with increasing mass velocity under sub-cooled boiling. However, the mass velocity is shown to be complex under nuclear boiling. In overall, the CHF decreases with mass velocity at low mass velocity, passes through a minimum, then increases at higher mass velocity. However it should be noted that the trend is not so clear. The minimum is found at about $3000\ \mathrm{kg\,m^{-2}\,s^{-1}}$. The liquid film thickness decreases, entrainment increases with increasing mass flux, which results in an early occurrence of CHF. From Fig. 12, we can also see that the CHF decreases with increasing critical quality. Moreover, the effect of critical quality with sub-cooled boiling is larger then nuclear boiling.

The overall trend of critical quality is shown in Fig. 13. The effect of critical quality on CHF at 10 MPa is represented in Fig. 13 for eight different mass velocities over a broad critical quality range of −0.5–0.9. In this figure, the results obtained by the GNN agree well with the database. In overall, the CHF decreases as the critical quality increases for low- and intermediate-quality regions as shown in Fig. 13. At high qualities, however, the CHF remains almost constant regardless of the quality increase.

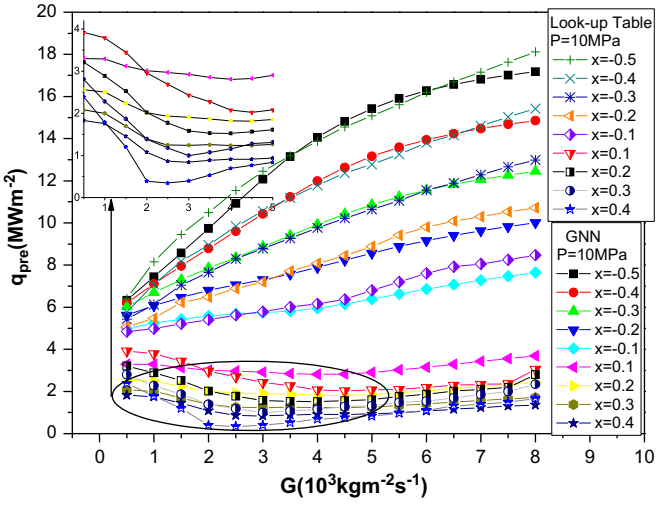

Fig. 12. Effect of mass flux on CHF for local conditions ($P = 10$ MPa).

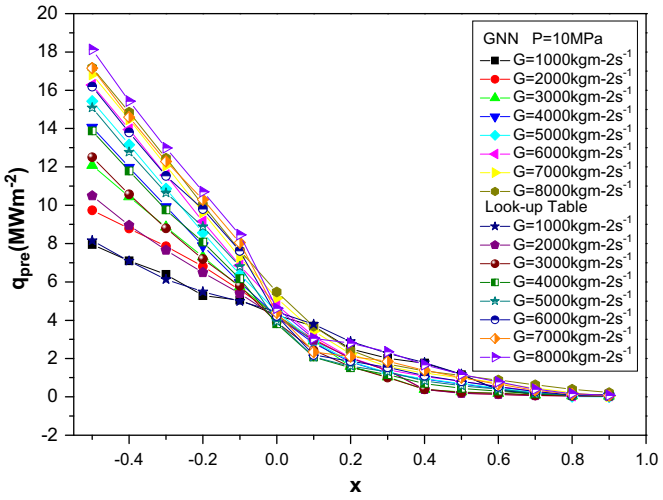

Fig. 13. Effect of critical quality on CHF for local conditions ($P = 10$ MPa).

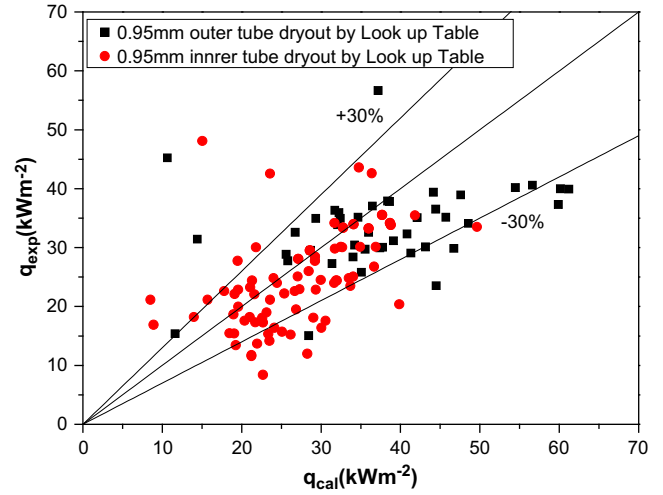

Fig. 14. Comparison between experimental data and calculation results by look-up table for 0.95 mm gap.

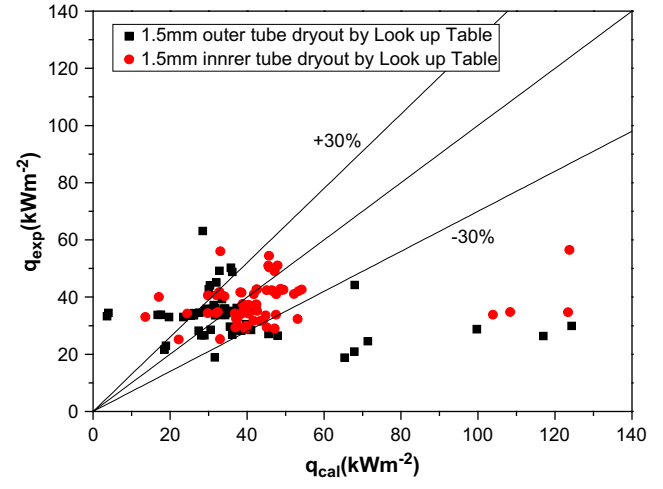

Fig. 15. Comparison between experimental data and calculation results by look-up table for 1.5 mm gap.

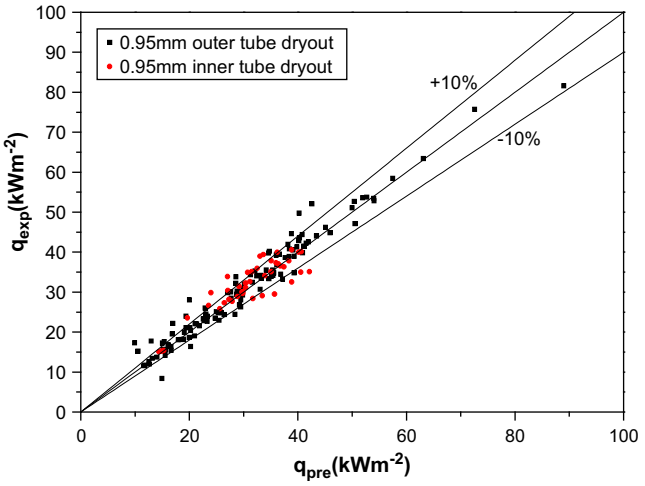

Fig. 16. Comparison between prediction results and experimental data for 0.95 mm gap.

7. Prediction of the CHF in vertical narrow annuli by GNN

In this section, prediction of dryout point is investigated by GNN with distilled water upflowing through narrow annular channel with 0.95 mm and 1.5 mm gaps, respectively. The GNN can be applied to the following ranges of flow: system pressure, 1.08–3.11 MPa; mass flux, 56.5–141.6 kg m^{-2} s^{-1}; steam quality, 0.694–0.987. The basic experimental apparatus are briefly introduced in Section 2. We obtained 301 experimental data [35]. In the following, the comparisons between the prediction results of the Groeneveld look-up table [30] and present data are firstly shown in Figs. 14 and 15. From Figs. 14 and 15, we can see there is a large deviation between them. The discrepancy can be attributed to the following reasons: While the Groeneveld look-up table is based on fairly sizeable experimental databases, the size of test tubes employed in their experiments is much larger then the narrow annuli. The equivalent diameter of narrow annuli is outside the applied range of Groeneveld look-up table. The inner and outer surfaces of narrow annuli affect with each other. Due to its particular structure geometry, mechanism of dryout in narrow annuli may be more complex than that of conventional round tubes and further study should be carried out. Next, the GNN is trained and

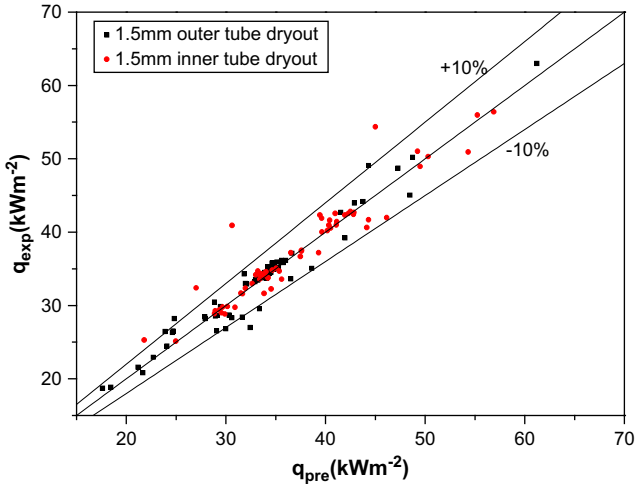

Fig. 17. Comparison between prediction results and experimental data for 1.5 mm gap.

tested based on those experimental data. Typically 75% of the experimental data was used for training and cross validation (60% for training and 15% for cross validation) and the rest 25% for testing. The mean square errors (MSE) of the training, validation and testing are all lower than 0.05148, 0.07263 and 0.06594, respectively. The trained GNN is used to predict CHF. The prediction results are as following Figs. 16 and 17. From Figs. 16 and 17, we can clearly find that the prediction results by GNN have a good agreement with experimental data. From the results, the MSE error of the prediction results are lower than 0.15.

8. Conclusions

A new method of predicting the CHF is proposed to use the fuzzy c-means clustering and the GNN. The GNN mode is constructed. The GNN mode has some advantages of its globe optimal searching, quick convergence speed and solving non-linear problem. The 2006 CHF look-up table [30] is successfully partitioned into five groups by using Fuzzy c-means (FCM) clustering algorithm according to the data characteristics. After classification of the data, The CHF data in each group are trained in a GNN to predict the CHF. Local condition type CHF data are predicted successfully on the basis of 6930 CHF data from the 2006 CHF look-up table [30]. The prediction results are consistent with database very well. The developed method can be used in numerous two-phase flow problems. In addition, the effects of main parameters such as system pressure, mass flow rate and equilibrium quality on CHF were analyzed using the GNN. The following conclusions are obtained: (1) The CHF decreases with increasing system pressure under sub-cooled boiling. The CHF increases with pressure at low pressures, passes through a maximum, then decreases at higher pressures under nuclear boiling. (2) The CHF increases with increasing mass velocity with sub-cooled boiling. The CHF decreases with mass velocity at low mass velocity, passes through a minimum, then increases at higher mass velocity under nuclear boiling. (3) The CHF decreases as the critical quality increases for low- and intermediate-quality regions. At high qualities, however, the CHF remains almost constant regardless of the quality increase. The results agree with practical behavior as it is generally understood. At last, the GNN is successfully applied to predict the CHF with distilled water flowing upward through narrow annular channel with 0.95 mm and 1.5 mm gaps, respectively. The GNN prediction results have a good agreement with experimental data. The proposed methodology allows us to achieve accurate results, thus it is suitable for the processing of the CHF data.

Acknowledgments

This work is supported by the Program for New Century Excellent Talents in University (NCET-06-0837) and by the National Natural Science Foundation of China (No.10675096 and No. 19675028).

References

[1] L.S. Tong, An evaluation of the departure from nucleate boiling in bundles of reactor fuel rods, Nuclear Science and Engineering 33 (1968) 7–15.
[2] D.H. Hwang, Y.J. Yoo, J.R. Park, Y.J. Kim, Evaluation of the thermal margin in a KOFA-loaded core by a multichannel analysis methodology, Journal of the Korean Nuclear Society 27 (1995) 518–531.
[3] G.P. Celata, M. Cumo, Y. Katto, A. Mariani, Prediction of the critical heat flux in water subcooled flow boiling using a new mechanistic approach, International Journal of Heat and Mass Transfer 42 (1999) 1457–1466.
[4] R.W. Bowring. A simple but accurate round tube, uniform heat flux, dryout correlation over the pressure range 0.7–17 mn/m, in AEEW-R. (1972) 789.
[5] Y. Fujita, Predictive methods of heat transfer coefficient and critical heat flux in mixture boiling, Experimental Heat Transfer Fluid Mechanics and Thermodynamics (1997) 831–842.
[6] D.C. Groeneveld, L.K.H. Leung, P.L. Kirillov, V.P. Bobkov, I.P. Smogalev, X.C. Vinogradov, V.N. Huang, E. Royer, The 1995 look-up table for critical heat flux in tubes, Nuclear Engineering and Design 163 (1996) 1–23.
[7] H.G. Kim, J.C. Lee, Development of a generalized critical heat flux correlation through the alternating conditional expectation algorithm, Nuclear Science and Engineering 127 (1997) 300–316.
[8] D.G. Lee, Critical heat flux prediction using genetic programming for water flow in vertical round tubes, International Communications in Heat and Mass Transfer 24 (1997) 919–929.
[9] J.H. Holland, Adaptation in Natural and Artificial Systems, University of Michigan, Ann Arbor, MI, 1975.
[10] L. Zadeh, Fuzzy sets, Information and Control 8 (3) (1965) 338–353.
[11] S.K. Moon, S.H. Chang, Classification and prediction of the critical heat flux using fuzzy clustering and artificial neural networks, Nuclear Engineering and Design 150 (1994) 151–161.
[12] Z. Michalewicz, Genetic Algorithms + Data Structures = Evolution Programs, second extended ed. Springer Verlag, New York, 1994.
[13] C. Darwin, The Origin of Species by Means of Natural Selection, John Murray, London, 1859.
[14] D.E. Goldberg, Genetic Algorithms in Search Optimization and Machine Learning, Addison Wesley, Reading, MA, 1989.
[15] M. Mitchell, An Introduction to Genetic Algorithms, MIT Press, Cambridge, MA, 1996.
[16] H. Peng, X. Ling, Optimal design approach for the plate-fin heat exchangers using neural networks cooperated with genetic algorithms, Applied Thermal Engineering 28 (5–6) (2008) 642–650.
[17] R. Ghorbani, Q. Wu, G.G. Wang, Nearly optimal neural network stabilization of bipedal standing using genetic algorithm, Engineering Applications of Artificial Intelligence 20 (4) (2007) 473–480.
[18] M. Delgado, M.C. Pegalajar, A multiobjective genetic algorithm for obtaining the optimal size of a recurrent neural network for grammatical inference, Pattern Recognition 38 (9) (2005) 1444–1456.
[19] T. Shin, I. Han, Optimal signal multi-resolution by genetic algorithms to support artificial neural networks for exchange-rate forecasting, Expert Systems with Applications 18 (4) (2000) 257–269.
[20] Z. Xiao, S.J. Ye, B. Zhong, C.X. Sun, BP neural network with rough set for short term load forecasting, Expert Systems with Applications 36 (1) (2009) 273–279.
[21] B.H.M. Sadeghi, A BP-neural network predictor model for plastic injection molding process, Journal of Materials Processing Technology 103 (3) (2000) 411–416.
[22] Q. Li, J.Y. Yu, B.C. Mu, X.D. Sun, BP neural network prediction of the mechanical properties of porous NiTi shape memory alloy prepared by thermal explosion reaction, Materials Science and Engineering A 419 (1–2) (2006) 214–217.
[23] J.Q. Yi, Q. Wang, D.B. Zhao, J.T. Wen, BP neural network prediction-based variable-period sampling approach for networked control systems, Applied Mathematics and Computation 185 (2) (2007) 976–988.
[24] S. Motlaghi, F. Jalali, M.N. Ahmadabadi, An expert system design for a crude oil distillation column with the neural networks model and the process optimization using genetic algorithm framework, Expert Systems with Applications 35 (4) (2008) 1540–1545.
[25] V.R. Adineh, C. Aghanajafi, G.H. Dehghan, S. Jelvani, Optimization of the operational parameters in a fast axial flow CW CO_2 laser using artificial neural networks and genetic algorithms, Optics & Laser Technology 40 (8) (2008) 1000–1007.
[26] S. Kim, H.S. Kim, Neural networks and genetic algorithm approach for nonlinear evaporation and evapotranspiration modeling, Journal of Hydrology 351 (3–4) (2008) 299–317.
[27] J.L. Xu. A genetic neural network for predicting materials mechanical properties, in: Third International Conference on Natural Computation (ICNC 2007) 1 (2007) 710–714.
[28] P.S. Heckerling, G.J. Canaris, S.D. Flach, T.G. Tape, R.S. Wigton, B.S. Gerber, Predictors of urinary tract infection based on artificial neural networks and genetic algorithms, International Journal of Medical Informatics 76 (4) (2007) 289–296.
[29] G.B. Sahoo, C. Ray, Predicting flux decline in crossflow membranes using artificial neural networks and genetic algorithms, Journal of Membrane Science 283 (1–2) (2006) 147–157.
[30] D.C. Groeneveld, J.Q. Shan, A.Z. Vasić, L.K.H. Leung, A. Durmayaz, J. Yang, S.C. Cheng, A. Tanase, The 2006 CHF look-up table, Nuclear Engineering and Design 237 (2007) 1909–1922.
[31] J.M. Keller, M.R. Gray, J.A. Givens, A fuzzy k-nearest neighbor algorithm, IEEE Transactions on System, Man and Cybernetics 15 (1985) 580–585.
[32] J.C. Bezdek, Pattern Recognition with Fuzzy Objective Function Algorithms, Plenum, M, New York, 1981.
[33] Z.R. Yuan, Artificial Neural Network and Its Applications, Tsinghua University Press, Beijing, 2000, pp. 118–119.
[34] H.M. Kottowski, C. Savatteri, W. Hufschmidt, A new critical heat flux correlation for boiling liquid metals, Nuclear Science and Engineering 108 (1991) 396–413.
[35] W.X. Tian, M. Aye, S.Z. Qiu, D.N. Jia, Study on dryout point in vertical narrow annuli, Nuclear Science and Techniques 16 (1) (2005) 53–58.
[36] M.E. Jefferson, N. Pendleton, C.P. Lucas, S.B. Lucas, M.A. Horan, Evolution of artificial neural network architecture: prediction of depression after mania, Methods of Information in Medicine 37 (1998) 220–225.